https://doi.org/10.1016/j.ijhydene.2020.05.266

Ni-doped A-site-deficient $La_{0.7}Sr_{0.3}Cr_{0.5}Mn_{0.5}O_{3-\delta}$ perovskite as anode of direct carbon solid oxide fuel cells

Weizi Cai[a,b], Mingyang Zhou[b], Dan Cao[b], Xiaomin Yan[b], Qing Li[a], Shengping Lü[a], Caiyun Mao[a], Yuzhi Li[a], Yongmin Xie[c], Caiwen Zhao[a], Jialing Yu[a], Meng Ni[d], Jiang Liu[b,*], Hailin Wang[a,**]

[a] College of Engineering, South China Agricultural University, Guangzhou 510640, PR China;

[b] Guangzhou Key Laboratory for Surface Chemistry of Energy Materials, New Energy Research Institute, School of Environment and Energy, South China University of Technology, Guangzhou 510006, PR China;

[c] School of Metallurgy and Chemical Engineering, Jiangxi University of Science and Technology, Ganzhou 341000, PR China

[d] Building Energy Research Group, Department of Building and Real Estate, The Hong Kong Polytechnic University, Hung Hom, Kowloon, Hong Kong 999077, PR China.

Abstract

A Ni-doped A-site-deficient $La_{0.7}Sr_{0.3}Cr_{0.5}Mn_{0.5}O_{3-\delta}$ perovskite (N-LSCM) was synthesized and systematically characterized towards the application as the anode

*Corresponding author:
Tel.: +86 20 22236168, Fax: +86 20 22236168, E-mail: **jiangliu@scut.edu.cn** (Prof. J. LIU)
Tel.: +86 20 85280221, Email: **hlwang@scau.edu.cn** (Prof. H. WANG)

electrode for direct carbon solid oxide fuel cells (DC-SOFCs). The microstructure and electrochemical properties of N-LSCM under the operation conditions of DC-SOFCs have been evaluated. An *in-situ* exsolution of Ni nanoparticles on the N-LSCM perovskite matrix is found, revealing a maximum power density of 153 mW cm^{-2} for the corresponding DC-SOFC at 850 °C, compared to 114 mW cm^{-2} of the cell with stoichiometric LSCM. The introduction of Ni nanoparticles exsolution and A-site deficient is believed to boost the formation of highly mobile oxygen vacancies and electrochemical catalytic activity, and further improves the output performance of the DC-SOFC. It thus promises as a suitable anode candidate for DC-SOFCs with whole-solid-state configuration.

Keywords Direct carbon solid oxide fuel cell; anode catalyst; strontium and manganese co-doped lanthanum chromites; *in situ* exsolution

1. Introduction

For a long time, energy crisis has been one of the most critical challenges facing mankind. Primary energy consumption grew at a rate of 2.9% and carbon emissions grew by 2.0% in 2018, which was the fastest growing rate since 2010. Fossil fuel, of which coal accounts for about 60 %, still holds major part of the world's energy markets. Unlike hydrogen, coal is one of the most abundant and frequently-used energy

resources in the earth, especially in China. Sadly, however, about half of the coal is directly combusted for electricity generation in China, resulting serious air pollution and climate impact. What's more, the energy conversion efficiency of coal-fired power plant is unsatisfactorily, meaning that huge amount of energy resources are wasted, while enormous pollutants are emitted to atmosphere. Novel clean coal technologies are urgently needed to replace the traditional thermal power technology and return the blue sky to people.

Direct carbon solid oxide fuel cell (DC-SOFC) is a whole-solid-state fuel cell, with a ceramic oxygen ion conductor as electrolyte, operating directly on solid carbon as fuel [1-7]. Different from other fuel cells, DC-SOFCs are able to generate electricity without any liquid medium or feeding gas, which avoid leakage and corrosion issues of high temperature liquid medium, simplify system deployment and administration, and reduce overall cost. The first DC-SOFC without any liquid medium was designed by Nakagawa and Ishida in 1988[8]. They believed that the operation mechanism of DC-SOFC was consisted of the electrochemical reaction of CO (1) and the Boudouard reaction (2):

$$CO + O^{2-} \rightarrow CO_2 + 2e^- \quad (1)$$

$$C + CO_2 \rightarrow 2CO \quad (2)$$

It had been verified by our group [9], through comparing the electrical performances and impedance spectra of an SOFC operated at carbon and CO, respectively. In the instant of DC-SOFC startup, CO dominates the equilibrium gas

composition in the anode chamber of the DC-SOFC, as CO is the favored product in a C-O system with excess carbon at high temperature of DC-SOFC operation. With the discharge of the DC-SOFC, CO firstly takes electrochemical reaction with O^{2-} on the anode of the DC-SOFC, and produces two electrons and CO_2 (Reaction 1). Spontaneously, the product, CO_2, would diffuse from the anode to the carbon fuel because of the concentration difference, and reacts with carbon to produce more CO (Reaction 2). Then, partial CO would diffuse back to the anode, while the other CO would be released from the system. During the whole process, CO and CO_2 can be perceived as vehicles, delivering the static solid carbon to the DC-SOFC. From another perspective, this process also can be regarded as internal gasification of solid carbon, which skillfully solves the mass transfer issues of solid carbon fuel. Discharge without necessary for carbon fuel to have any physical or chemical contact with the anode of the cell is the most significant feature and superiority to other types of direct carbon fuel cells. Accordingly, the strategies for improving the output performance of DC-SOFC should be focused on catalyzing both of reaction (1) and (2). Tang et al. had tried to apply catalysts to promote the electrochemical reaction and Boudouard reaction of DC-SOFCs and successfully improved the performance [1]. Silver-Gadolinium doped ceria (GDC, $Gd_{0.2}Ce_{0.8}O_{1.9}$) composed anode material was applied to catalyze the electrochemical reaction of CO and Fe was loaded on activated carbon fuel to catalyze the Boudouard reaction, respectively. It effectively enhanced the output performance of DC-SOFC from a maximum power density of 4 mW cm^{-2} to 46 mW cm^{-2} at 800 °C. In fact, the Boudouard

reaction catalysts have been widely studied for decades. Apart from Fe-based catalysts, other transition metals, alkali metals and alkaline-earth metals also have been developed as Boudouard reaction catalysts, like Li, K, Ca, Ni and so on [2, 10, 11]. Hence, the promoted effects of these Boudouard reaction catalysts on the DCFC performance are investigated systematically. Nevertheless, the studies on the anode catalysts for the electrochemical oxidation of CO for DC-SOFC are still too few to provide a desirable output performance, comparing to that of the conventional hydrogen SOFC (>1000 mW/cm^2 at 800 °C). Therefore, studying and designing an anode material with excellent electrocatalytic activity for electrochemical oxidation of CO is one of the major critical scientific challenges for DC-SOFCs. Moreover, common requirements for an anode of SOFC are applicable for that of DC-SOFC, such as adequate electronic and ionic conductivity, thermal expansion compatibility, high porosity and capacity to prevent coke and resist sulfur.

As the most widely used traditional anode of SOFC, Ni-YSZ had been applied as the anode of a DC-SOFC stack with a configuration of three cells in series [12]. Powered by 5 wt. % Fe-loaded activated carbon fuel, the DC-SOFC stack with a total effective area of 5.4 cm^2 offered an open circuit voltage of 3 V and a peak power of 2.4 W. Infiltrating Cu particles on the Ni-YSZ surface, Dudek et al. found that the DC-SOFC with Cu-Ni-YSZ anode performed better than that with Ni-YSZ anode. The maximum power density of 118 mW cm^{-2} was reached for DC-SOFC with Cu-Ni-YSZ anode at 800 °C, comparing to 96 mW cm^{-2} obtained by DC-SOFC with Ni-YSZ anode

105 [13]. Besides metal-based anode, perovskite material also had been developed as an
106 anode for DC-SOFC. Xiao et al. investigated the electrocatalytic activity of
107 $SrFe_{0.75}Mo_{0.25}O_3$-$La_{0.9}Sr_{0.1}Ga_{0.8}Mg_{0.2}O_3$ composed anode and the output performance
108 of the corresponding DC-SOFC (405 mW cm^{-2}, 850 °C), which is comparable to that
109 of a Ni-based DC-SOFC[14]. Recently, Lü et al. studied a Nb-doped $La_{0.8}Sr_{0.2}FeO_3$
110 perovskite oxide as anode of DC-SOFC fueled by activated carbon and corn straw
111 derived carbon [15]. The DC-SOFCs with Nb-doped $La_{0.8}Sr_{0.2}FeO_3$ anode
112 demonstrated peak power densities of 302.8 mW cm^{-2} and 218.5 mW cm^{-2}, when fueled
113 by activated carbon and corn straw carbon at 850 °C, respectively. The output
114 performances of the DC-SOFCs are desirable and the result of this study is impressive,
115 which demonstrates the feasibility and the advantage of perovskite anode material for
116 DC-SOFCs. The perovskite strontium and manganese co-doped lanthanum chromites
117 (LSCM) have been widely investigated as promising SOFC anode materials with high
118 anodic performance and excellent redox stability [16-18]. However, poor
119 electrochemical catalytic property and low ionic conductivity are the critical
120 bottlenecks of the lanthanum chromites ($LaCrO_3$) based materials as the SOFC anode.
121 Recently, *in situ* exsolution of metallic nanoparticles on perovskite is regarded as an
122 effective way to generate well-dispersed nanoparticle with high catalytic activity. *In*
123 *situ* exsolutions of Ni, Fe, Co nanoparticles or Ni-Fe, Co-Fe alloy particles on
124 perovskite oxides have demonstrated an excellent catalytic activity as SOFCs anode
125 operated on hydrogen and sulfur containing alkane gas [19-22].

However, to the best of our knowledge, few works have been done so far to assess the electrochemical performance of perovskite anode with nanoparticles *in situ* exsolution in DC-SOFCs. In this work, a Ni-doped A-site-deficient LSCM perovskite oxide was synthesized and systematically characterized towards the application as the anode electrode for DC-SOFCs. The detailed structure and electrochemical properties of Ni-doped A-site-deficient LSCM was specifically investigated, which was hoped to be able to address the critical scientific challenges of DC-SOFCs.

2. Experimental

2.1. Materials preparation

The anode materials of $La_{0.7}Sr_{0.3}Cr_{0.5}Mn_{0.5}O_{3-\delta}$ and A-site-deficient $La_{0.7}Sr_{0.3}Cr_{0.5}Mn_{0.5}Ni_{0.1}O_{3-\delta}$, denoted as LSCM and N-LSCM respectively, were synthesized via EDTA-citrate sol-gel process. Stoichiometric amounts of $La(NO_3)_3 \cdot 6H_2O$ (A.R., Sinopharm Chemical Reagent Co., Ltd. China), $Sr(NO_3)_2$ (A.R., Sinopharm Chemical Reagent Co., Ltd. China), $Mn(NO_3)_2 \cdot 6H_2O$ (A.R., Sinopharm Chemical Reagent Co., Ltd. China), $Cr(NO_3)_3 \cdot 9H_2O$ (A.R., Tianjin kemio Chemical Reagent Co., Ltd. China) and $Ni(NO_3)_2 \cdot 6H_2O$ (A.R., Tianjin kemio Chemical Reagent Co., Ltd. China) were used as the source materials and dissolved in deionized water under stirring, following by adding EDTA (A.R., Sinopharm Chemical Reagent Co., Ltd. China) and citric acid (A.R., Sinopharm Chemical Reagent Co., Ltd. China) into the mixed solution with a molar ratio of 1:1:2 for total metal ions: EDTA: citric acid.

Then, ammonia (25 wt.%, Guangzhou Chemical Reagent Factory, China) was applied to retain the pH value of the solution in the range of 7-8, following by heat-treatment at 100 °C under stirring. As the water content decreased, a transparent gel was obtained, and it was pre-fired at 250 °C to become a solid precursor. Finally, the as-prepared solid precursor was calcined at 1000 °C for 4 hours in air to obtain pure perovskite phase. The LSCM and N-LSCM samples were exposed to carbon monoxide atmosphere at 850 °C for 24 hours. The LSCM and N-LSCM after reduction were denoted as R-LSCM and R-N-LSCM, respectively. Yttrium stabilized zirconia, (YSZ, Tosoh Corporation, Japan), $(La_{0.60}Sr_{0.40})_{0.95}Co_{0.20}Fe_{0.80}O_{3-\delta}$ (LSCF-P, Fuel Cell Materials Inc., USA), and $Gd_{0.1}Ce_{0.9}O_{2-\delta}$ (GDC10-HP, Fuel Cell Materials Inc., USA) were directly used as electrolyte material and composed cathode materials, respectively.

For the carbon fuel, Fe-loaded activated carbon had been demonstrated as an excellent carbon fuel for a DC-SOFC [1, 3, 23]. Therefore, in this work, Fe-loaded activated carbon was chosen as carbon fuel and prepared using impregnation method, as has been reported elsewhere. To prepare 5 wt. % Fe-loaded carbon fuel, 3.62 g of $Fe(NO_3)_3 \cdot 9H_2O$ was dissolved in deionized water. Then, 10 g of pure activated carbon powder was added into the $Fe(NO_3)_3 \cdot 9H_2O$ solution under stirring for 1 hour, followed by heat treatment at 80 °C till the solvent was evaporated. Finally, the carbon fuel was heated at 700 °C for 1 hour under N_2 atmosphere to decompose the nitrate.

2.2. Fuel cell fabrication

The single cells studies in this work were YSZ electrolyte supported cells, and the electrodes were prepared by spray deposition technique [24]. YSZ electrolyte substrates were fabricated by dry-pressing YSZ powder uniaxially under 200 MPa, followed by sintering at 1400 °C for 4 hours. After heat treatment, the thickness of the YSZ electrolyte was about 300 μm with a diameter of about 11 mm. To increase the oxygen ionic conductivity of the anode, LSCM was mixed with equivalent YSZ powders to get LSCM-YSZ composed anode. Glycol, ethylene glycol and isopropyl alcohol were premixed with the electrode powders (50 wt.% LSCM- 50 wt.% YSZ), using a high-energy ball grinder (Fritsch, Pulverisette 6) at a rotational speed of 400 rpm for 30 min to obtain an uniform colloidal suspension, which was then deposited on one side of the YSZ electrolyte pellets by a spray gun. Then, the cells were fired at 1000 °C in air for 4 hours. Finally, a composed cathode suspension (40%LSCF-60%GDC) was deposited on the other side of the YSZ pellets via spray deposition technique and fired at 900 °C in air for 2 hours to obtain the single cell with LSCM-YSZ/YSZ/LSCF-GDC configuration. The effective surface area of the cathode was 0.28 cm^2.

2.3. Material characterization

An X-ray diffractometer (XRD, Rigaku D/max-IIIA diffractometer, Japan, Cu-Ka radiation, operated at 35 kV, 30 mA, l = 1.54184 Å) was employed to confirm the crystalline structures of sample. The step scanning of the diffraction data was in the 2θ

range of 20-80˚ with intervals of 0.02˚. Cold field scanning electron microscope (SEM, Hitachi SU8010) was used to observe the microstructures and chemical compositions of the specimens.

2.4. Cell assembling and characterization

Single cells were sealed to one end of a quartz tube with silver paste for fuel cells test. Silver wires were attached to the anode and cathode, and connected to a Solartron 1287 potentiostat and a Solartron 1260 frequency response analyzer over the temperature range of 750–850 °C. Impedance spectra were acquired under open circuit voltage (OCV) conditions in a frequency range from 1 MHz to 0.1 Hz with an AC amplitude of 10 mV. For the cells operated on humidified hydrogen, the flow rate of fuel gases was 40 mL min^{-1}. For the cells operated on carbon fuel, 0.4 g Fe-loaded carbon fuel was filled into each cell. In all the testing experiment, the cathode side of the cells was exposed to ambient air. The schematic illustration of DC-SOFC testing has been reported in our previous works [23].

3. Results and discussion

3.1. XRD analysis and microstructure of the anode

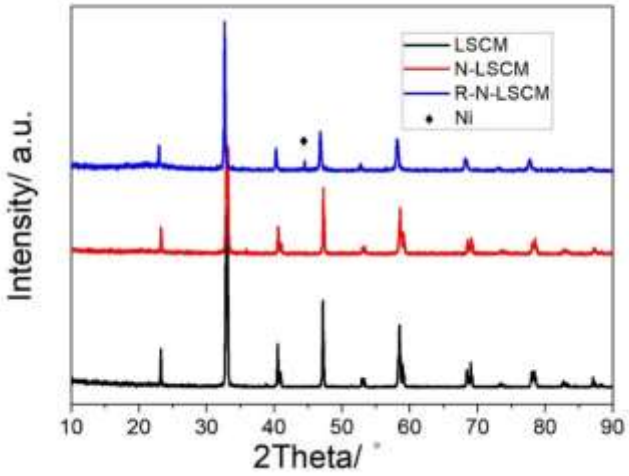

Fig. 1 – XRD patterns of the as-prepared LSCM and N-LSCM; and R-N-LSCM annealed in CO atmosphere at 850 °C.

Fig. 1 shows the XRD patterns of as-prepared LSCM and N-LSCM sintered at 1000 °C in air, which match those of the standard perovskite structure. No any undesired peaks can be observed, indicating high purity of the as-prepared LSCM and N-LSCM samples, and the successfully doping of Ni into the B-site of LSCM perovskite structure. The A-site-deficient N-LSCM still remains a single-phased perovskite structure, even being reduced in CO atmosphere at 850 °C for 24 hours. A peak ascribed to metallic Ni could be found around 45°, indicating the exsolution of metallic Ni. What's interesting, we find a slight movement to lower diffraction angle of N-LSCM after reduction, which could be attributed to the following reasons. Firstly, under a reduction condition, parts of high valence B-site ions of N-LSCM could be reduced to low valence ions. The ionic radii of low valence ions are larger than that of high valence ions. Therefore, a larger B-site ionic would result in an increased lattice parameter and an increased interplanar distance of perovskite material. Secondly, a

reduction atmosphere would significantly enhance the oxygen vacancy concentration, and further lead to a lattice expansion of perovskite material and movement of XRD pattern to low diffraction angle, according to the Scherrer formula.

The microstructures of the as-prepared LSCM and N-LSCM samples after reduction (R-LSCM, R-N-LSCM) in CO atmosphere are shown in Fig. 2. The average particle size of R-LSCM is about 0.2- 2.0 μm, as well as R-N-LSCM. However, as shown in Fig. 2(d), lots of Ni nanoparticles were found on the surface of R-N-LSCM, comparing to the clean and smooth surface of R-LSCM (Fig. 2c). The Ni nanoparticles (~30 nm) are evenly exsolved and distributed on the perovskite matrix, which might play an important role in catalyzing the electrochemical reaction of CO. The cross-section microstructure of the N-LSCM anode layer on the whole fuel cell is also revealed in Fig. 3. The anode layer, with a thickness of 35 μm, closely attaches to the YSZ electrolyte substrate. In addition, the anode is fairly porous with relatively uniform microstructure.

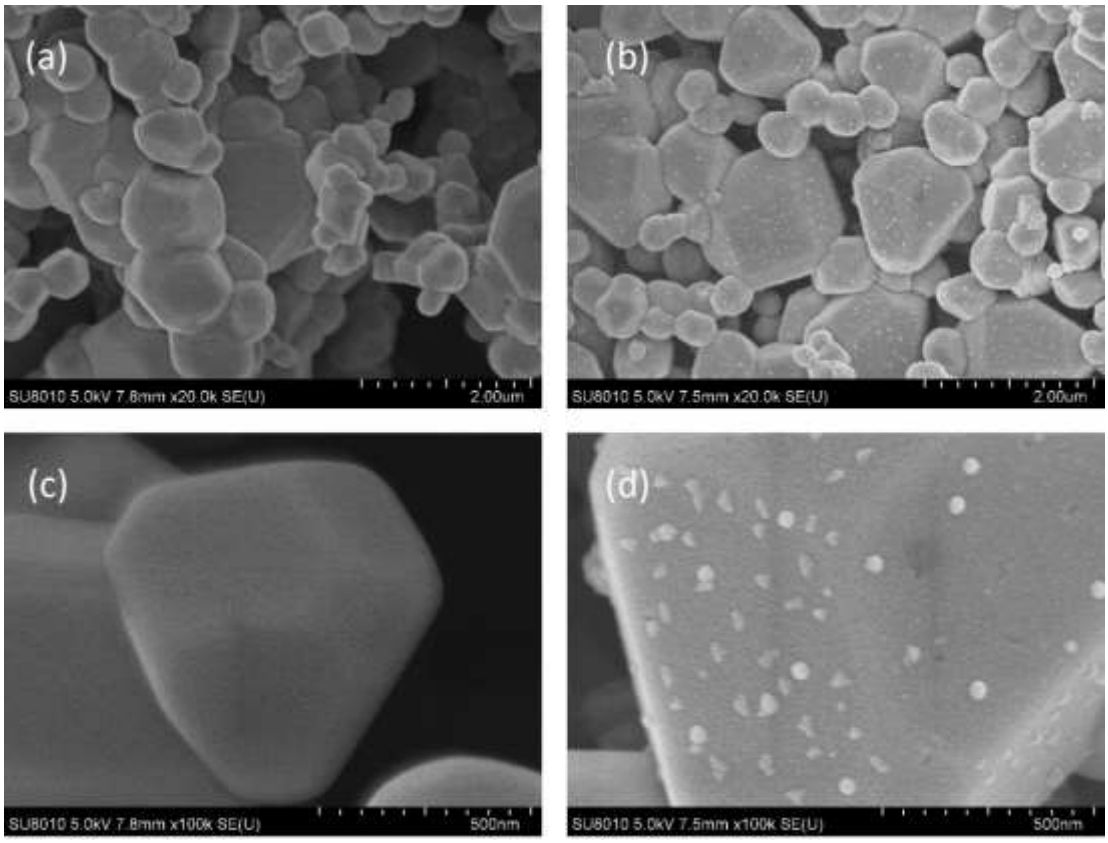

Fig. 2 – SEM pictures of the R-LSCM (a and c) and R-N-LSCM (b and d) samples, which were reduced in CO atmosphere at 850 °C for 24 hours.

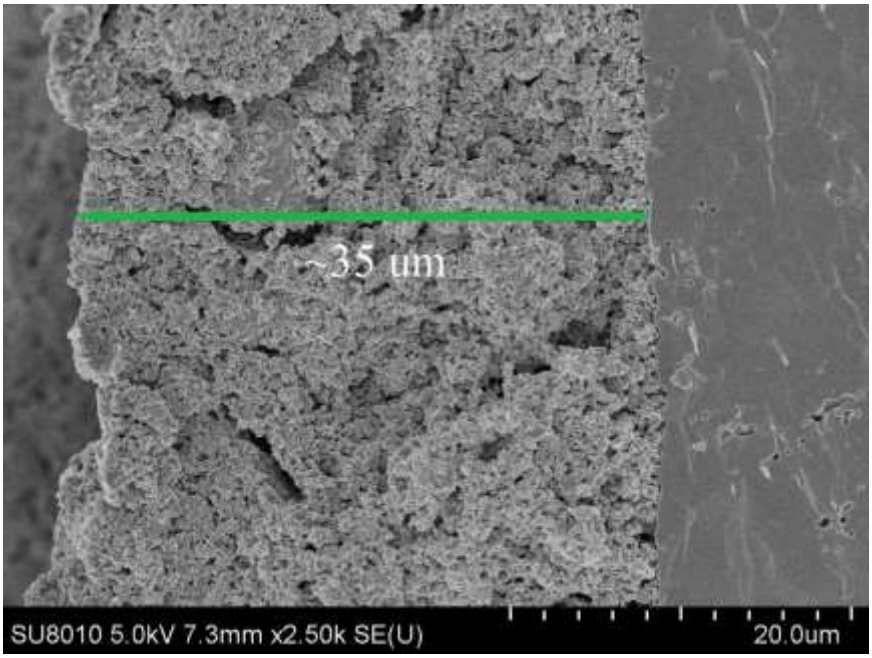

Fig. 3 – SEM picture of cross-section of the N-LSCM anode.

3.2. Electrochemical performance of the cells

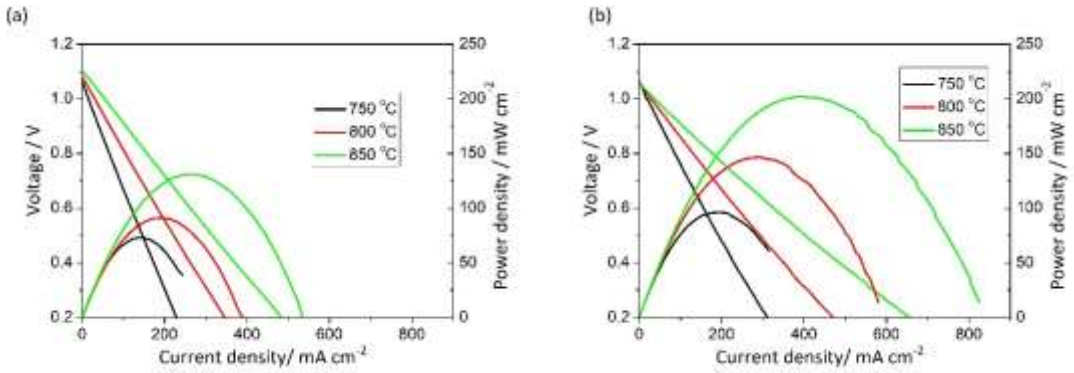

Fig. 4 – Output performances of LSCM (a) and N-LSCM (b) anode SOFC using humidified hydrogen (3 vol.% H_2O) as fuel.

The electrochemical performances of the LSCM and N-LSCM SOFC at 750-850 °C are evaluated using humidified hydrogen (3 vol.% H_2O) as fuel. An open circuit voltage greater than 1 V is achieved for both of the cells, indicating that the YSZ electrolyte is dense and the seal between the cells and connector is fine. Apparently, the output performances of the cell with N-LSCM anode are significantly higher than that of the cell with LSCM anode. The N-LSCM SOFC provides a maximum power density of 202 mW cm^{-2} at 850 °C, comparing to a maximum power density of 131 mW cm^{-2} attributed to the LSCM SOFC (Fig. 4).

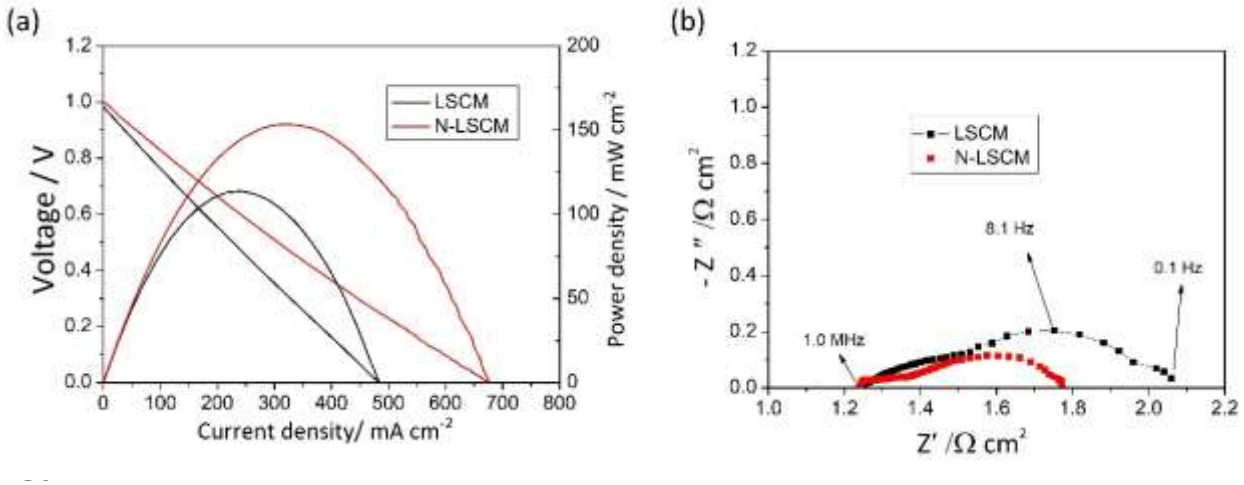

Fig. 5 – Output performance (a) and impedance spectra (b) of the DC-SOFCs with LSCM and N-LSCM anode at 850 °C.

Table 1 – Electrochemical properties of the DC-SOFCs at 850 °C with LSCM and N-LSCM anode, respectively.

	Open circuit voltage / V	Maximum power density/ mW cm^{-2}	Polarization resistance/ Ω cm^2	Total resistance/ Ω cm^2	Fuel utilization
LSCM	0.98	114	0.83	2.07	24.6
N-LSCM	1.0	153	0.54	1.78	33.6

The electrochemical performances of the LSCM and N-LSCM are further evaluated as the anodes of DC-SOFC (Table 1). It has been reported that the output performance of a DC-SOFC can be effectively enhanced through loading Fe catalyst on the carbon fuel to promote the Boudouard reaction rate. [1, 23] Therefore, in this work, 5 wt. % Fe-loaded activated carbon is used as the carbon fuel for DC-SOFCs. In addition, a DC-SOFC is more suitable to operate at high temperature above 850 °C, as CO is the favor product instead of CO_2 at high temperature in a C-O system with excess

amount of carbon. Moreover, limited to the practical conditions, we use silver wires as current wires in this experiment, and the melting point of silver is only about 960 °C. Accordingly, we just compare the output performances of the cells at 850 °C. As can be seen from Fig. 5(a), the N-LSCM DC-SOFC gives a maximum power density of 153 mW cm^{-2}, which is lower than that operated on humidified hydrogen (202 mW cm^{-2}) and obviously higher than that of LSCM DC-SOFC (114 mW cm^{-2}). Both of the open circuit voltages are about 1.0 V. At the same time, the electrochemical impedance spectra of the DC-SOFCs measured at open circuit voltage are shown in Fig. 5(b). The ohmic resistances of the two cells are also similar, due to the same YSZ electrolyte thickness and operating temperature. However, the polarization resistances of the cells are different, which further demonstrates the preferable electrocatalytic activity of N-LSCM for the electrooxidation of CO, comparing to that of LSCM. The enhanced electrocatalytic activity of N-LSCM could be attributed to the following reasons. Firstly, *in-situ* exsolution of Ni nanoparticles has been confirmed as an effective way to improve the electrocatalytic activity [19, 20, 25], taking the advantage of the introduction of A-site deficiency, which alters the stoichiometric composition to help the exsolution of Ni in the B-site. Secondly, lots of researches have demonstrated that doping Ni in the B-site of LSCM perovskite improves catalytic properties, electronic conductivity and ionic conductivity, and hence improved power density[26]. Thirdly, the introduction of A-site deficiency into the perovskite oxide is believed to increase oxygen vacancies and further promote the ionic conductivity [27].

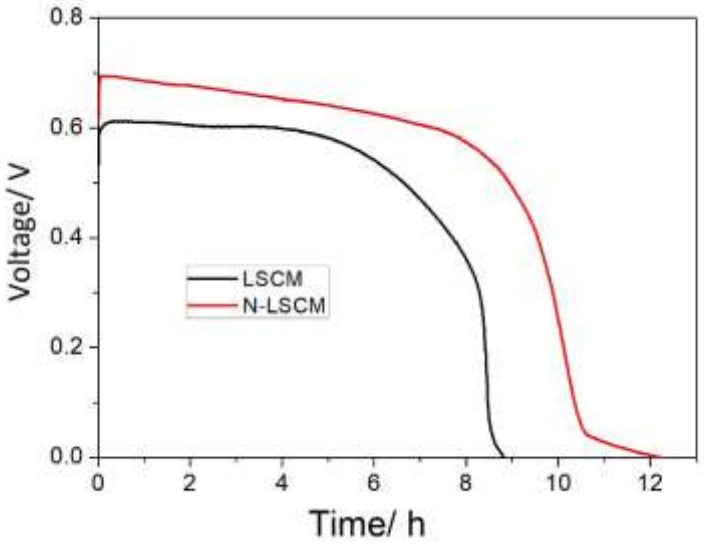

Fig. 6 – Discharging test of the LSCM and N-LSCM DC-SOFCs operated at a constant current of 50 mA at 850 °C.

Shown in Fig. 6 are the discharging curves of the DC-SOFCs with LSCM and N-LSCM anode, respectively. Both of the discharging curves discharge stably in the early stage, and then slowing quickly drop to 0 V. It could be attributed to the consumption of the carbon fuel and decline of the Fe catalyst. Powered by 5 wt.% Fe-loaded activated carbon, both of the cells discharge at a constant current of 50 mA(180 mA cm^{-2}). The discharging plateau (0.7 V) and discharging time (12.0 h) of the N-LSCM DC-SOFC are higher than those of the LSCM one (0.61 V and 8.8 h). The fuel utilization of DC-SOFC discharged with constant current can be calculated by the following formula [14]:

$$\eta = ItM_c/(95\%nm\mathrm{F}) \quad (3)$$

Here, η is fuel utilization, I is discharging current, t is discharging time, M_c is molar mass of carbon, n is molar number (n= 2), m is the mass of the carbon fuel, F is

the Faraday constant. For a discharging test of 12.0 hours and constant current of 50 mA, the released electric quantity is calculated as 2160 C according to the coulomb law. Therefore, according to the formula (3), the fuel utilizations through electrochemical oxidation of LSCM and N-LSCM DC-SOFCs are 24.6% and 33.6%, respectively.

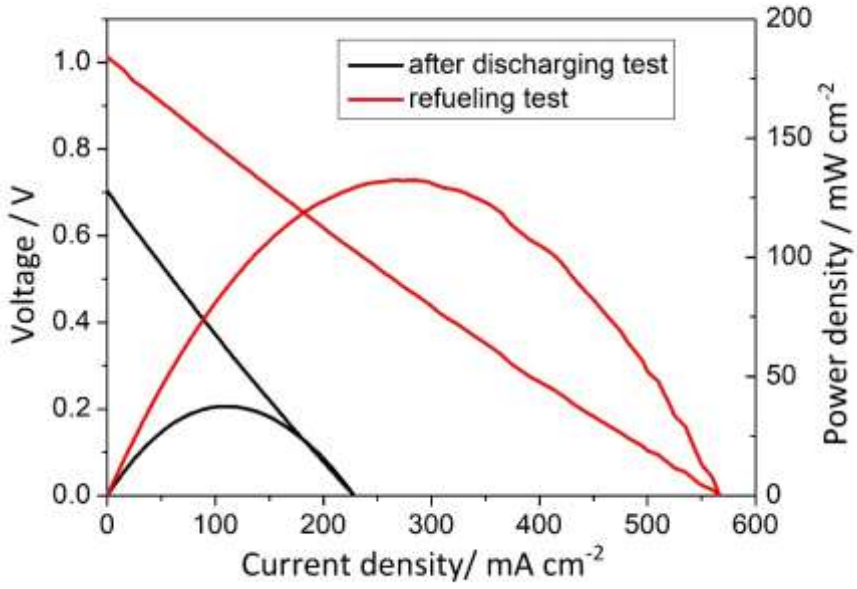

Fig. 7 – Output performance of the N-LSCM DC-SOFC after the discharging test and refueling more Fe-loaded carbon.

Fig. 7 shows the typical I-V-P curves of the N-LSCM DC-SOFCs after the discharging test. As can be seen, the open circuit voltage of the cell declines from 1 V to 0.7 V and the maximum power density decreases to 37 mW cm^{-2}. The fading open circuit voltage and power density are not because of the sintering or deactivation of the anode materials, as the discharging test only maintains for about 24 hours. The decayed output performance of the cell can be attributed to the decrease of the CO production

rate (the Boudouard reaction), which is caused by the consumption of the carbon fuel and the decline of the Boudouard reaction catalyst [14, 28]. To further confirm, the initial DC-SOFC was cooled down to room temperature and refueled with the same amount of Fe-loaded carbon fuel, and retested the output performance at 850 °C. For experiment in lab, when the carbon is used up, the DC-SOFC may be cooled down to room temperature. Then, the rubber stopper and ceramic cotton is removed and carbon is filled into the DC-SOFC. For practical use, the design has to be improved, with carbon fuel inlet and residue outlet, to enable carbon refuel during operation. As shown in Fig. 7, the open circuit voltage of the cell recovers to 1 V, and the power density peak of the cell is 133 mW cm^{-2}, which is just slightly lower than that of the cell before discharging test (153 mW cm^{-2}). There results prove that the degradation performance of the cell is mainly because of the carbon fuel consumption rather than the deactivation of the anode materials [2, 28, 29].

4. Conclusions

A Ni-doped A-site-deficient LSCM perovskite was synthesized and systematically characterized towards the application as the anode electrode for DC-SOFCs. Under the operation conditions of DC-SOFCs, an exsolution of Ni nanoparticles from the LSCM matrix was found to play a key role in enhancing the electrochemical catalytic activity, and hence improved the output performance of DC-SOFC significantly. The SOFCs with N-LSCM anode operated on hydrogen and Fe-loaded activated carbon provide

maximum power densities of 202 mW cm^{-2} and 153 mW cm^{-2} at 850 °C, respectively. The evenly dispersed and distributed Ni nanoparticles are believed to provide more active sites for the electrochemical oxidation reaction of CO and promote the electrochemical performance of the corresponding DC-SOFC. The DC-SOFC after discharging test can regain its initial output performance with reloaded carbon fuel. The LSCM perovskite with *in-situ* exsolution of Ni nanoparticles is demonstrated to be a promising anode for DC-SOFCs.

Acknowledgements

This work was supported by the National Science Foundation of China (NSFC, No. 91745203, 51904136 and U1601207), the Special Funds of Guangdong Province Public Research and Ability Construction (No. 2014A010106008), Science and Technology planning project of Guangdong Province (No.2017B010122001). M. Ni thanks the grant (Project Number: PolyU 152214/17E and PolyU 152064/18E) from Research Grant Council, University Grants Committee, Hong Kong SAR.

References

[1] Tang Y, Liu J. Effect of anode and Boudouard reaction catalysts on the performance of direct carbon solid oxide fuel cells. Int J Hydrogen Energy 2010;35:11188-93.

[2] Cai W, Liu J, Yu F, Zhou Q, Zhang Y, Wang X, Liu M, Ni M. A high performance direct carbon solid oxide fuel cell fueled by Ca-loaded activated carbon. Int J Hydrogen Energy 2017;42:21167-76.

363 [3] Cai W, Zhou Q, Xie Y, Liu J, Long G, Cheng S, Liu M. A direct carbon solid oxide
364 fuel cell operated on a plant derived biofuel with natural catalyst. Appl Energy
365 2016;179:1232-41.
366 [4] Liu J, Zhou M, Zhang Y, Liu P, Liu Z, Xie Y, Cai W, Yu F, Zhou Q, Wang X.
367 Electrochemical oxidation of carbon at high temperature: principles and applications.
368 Energy fuel 2017;32:4107-17.
369 [5] Zhou M, Wang X, Zhang Y, Qiu Q, Liu M, Liu J. Effect of counter diffusion of CO
370 and CO2 between carbon and anode on the performance of direct carbon solid oxide
371 fuel cells. Solid State Ionics 2019;343:115127.
372 [6] Wu H, Xiao J, Zeng X, Li X, Yang J, Zou Y, Liu S, Dong P, Zhang Y, Liu J. A high
373 performance direct carbon solid oxide fuel cell–A green pathway for brown coal
374 utilization. Appl Energy 2019;248:679-87.
375 [7] Cao T, Huang K, Shi Y, Cai N. Recent advances in high-temperature carbon–air fuel
376 cells. Energy Environ Sci 2017;10:460-90.
377 [8] Nakagawa N, Ishida M. Performance of an internal direct-oxidation carbon fuel cell
378 and its evaluation by graphic exergy analysis. Ind Eng Chem Res 1988;27:1181-5.
379 [9] Xie Y, Tang Y, Liu J. A verification of the reaction mechanism of direct carbon solid
380 oxide fuel cells. J Solid State Electr 2013;17:121-7.
381 [10] Wu Y, Su C, Zhang C, Ran R, Shao Z. A new carbon fuel cell with high power
382 output by integrating with in situ catalytic reverse Boudouard reaction. Electrochem
383 Commun 2009;11:1265-8.
384 [11] Jiao Y, Tian W, Chen H, Shi H, Yang B, Li C, Shao Z, Zhu Z, Li S-D. In situ
385 catalyzed Boudouard reaction of coal char for solid oxide-based carbon fuel cells with
386 improved performance. Appl Energy 2015;141:200-8.
387 [12] Bai Y, Liu Y, Tang Y, Xie Y, Liu J. Direct carbon solid oxide fuel cell—a potential

high performance battery. Int J Hydrogen Energy 2011;36:9189-94.

[13] Tomov R, Dudek M, Hopkins S, Krauz M, Wang H, Wang C, Shi Y, Tomczyk P, Glowacki B. Inkjet Printing of Direct Carbon Solid Oxide Fuel Cell Components. ECS Transac 2013;57:1359-69.

[14] Xiao J, Han D, Yu F, Zhang L, Liu J, Zhan Z, Zhang Y, Dong P. Characterization of symmetrical $SrFe_{0.75}Mo_{0.25}O_{3-\delta}$ electrodes in direct carbon solid oxide fuel cells. J Alloy Compd 2016;688:939-45.

[15] Li J, Wei B, Wang C, Zhou Z, Lü Z. High-performance and stable $La_{0.8}Sr_{0.2}Fe_{0.9}Nb_{0.1}O_{3-\delta}$ anode for direct carbon solid oxide fuel cells fueled by activated carbon and corn straw derived carbon. Int J Hydrogen Energy 2018.

[16] Liu J, Madsen BD, Ji Z, Barnett SA. A fuel-flexible ceramic-based anode for solid oxide fuel cells. Electrochem solid ST 2002;5:A122-A4.

[17] Kim G, Lee S, Shin J, Corre G, Irvine J, Vohs J, Gorte RJ. Investigation of the structural and catalytic requirements for high-performance SOFC anodes formed by infiltration of LSCM. Electrochem solid ST 2009;12:B48-B52.

[18] Boulfrad S, Cassidy M, Djurado E, Irvine JTS, Jabbour G. Pre-coating of LSCM perovskite with metal catalyst for scalable high performance anodes. Int J Hydrogen Energy 2013;38:9519-24.

[19] Sun Y, Li J, Cui L, Hua B, Cui S, Li J, Luo J. A-site-deficiency facilitated in situ growth of bimetallic Ni–Fe nano-alloys: a novel coking-tolerant fuel cell anode catalyst. Nanoscale 2015;7:11173-81.

[20] Sun Y, Li J, Zeng Y, Amirkhiz BS, Wang M, Behnamian Y, Luo J. A-site deficient perovskite: the parent for in situ exsolution of highly active, regenerable nano-particles as SOFC anodes. J Mater Chem A 2015;3:11048-56.

[21] Yang C, Li J, Lin Y, Liu J, Chen F, Liu M. In situ fabrication of CoFe alloy nanoparticles structured $(Pr_{0.4}Sr_{0.6})_3(Fe_{0.85}Nb_{0.15})_2O_7$ ceramic anode for direct

414 hydrocarbon solid oxide fuel cells. Nano Energy 2015;11:704-10.

415 [22] Yang C, Yang Z, Jin C, Xiao G, Chen F, Han M. Sulfur-Tolerant Redox-Reversible
416 Anode Material for Direct Hydrocarbon Solid Oxide Fuel Cells. Adv mater
417 2012;24:1439-43.

418 [23] Cai W, Zhou Q, Xie Y, Liu J. A facile method of preparing Fe-loaded activated
419 carbon fuel for direct carbon solid oxide fuel cells. Fuel 2015;159:887-93.

420 [24] Dong F, Chen D, Chen Y, Zhao Q, Shao Z. La-doped $BaFeO_{3-delta}$ perovskite as a
421 cobalt-free oxygen reduction electrode for solid oxide fuel cells with oxygen-ion
422 conducting electrolyte. J Mater Chem 2012;22:15071-9.

423 [25] Thommy L, Joubert O, Hamon J, Caldes M-T. Impregnation versus exsolution:
424 Using metal catalysts to improve electrocatalytic properties of LSCM-based anodes
425 operating at 600 °C. Int J Hydrogen Energy 2016;41:14207-16.

426 [26] Tao S, Irvine JT. Synthesis and Characterization of $(La_{0.75}Sr_{0.25})Cr_{0.5}Mn_{0.5}O_{3-\delta}$,
427 a Redox-Stable, Efficient Perovskite Anode for SOFCs. J electrochem soc
428 2004;151:A252-A9.

429 [27] Ge L, Zhou W, Ran R, Liu S, Shao Z, Jin W, Xu N. Properties and performance of
430 A-site deficient $(Ba_{0.5}Sr_{0.5})_{1-x}Co_{0.8}Fe_{0.2}O_{3-\delta}$ for oxygen permeating membrane. J
431 Membrane Sci 2007;306:318-28.

432 [28] Cai W, Liu J, Xie Y, Xiao J, Liu M. An investigation on the kinetics of direct carbon
433 solid oxide fuel cells. J Solid State Electr 2016;20:2207-16.

434 [29] Yu F, Zhang Y, Yu L, Cai W, Yuan L, Liu J, Liu M. All-solid-state direct carbon
435 fuel cells with thin yttrium-stabilized-zirconia electrolyte supported on nickel and iron
436 bimetal-based anodes. Int J Hydrogen Energy 2016;41:9048-58.

437